

DC MOTOR HYBRID EQUIVALENT CIRCUIT MODEL AND NUMERICAL SIMULATION

Ning CHUANG, Timothy J. GALE and Richard LANGMAN

School of Engineering, University of Tasmania, Hobart, Tasmania, Australia

Ph. +61 (0)3 62262753, E-mail: T.Gale@utas.edu.au

Abstract: *This paper describes an example implementation illustrating methods for the derivation, SIMULINK implementation and educational application of complete circuit DC machine models and related methods for measuring machine parameters. The model represents the complete electric circuit including all armature and field coils and two different equivalent circuits allowing for the switching action of commutation. It is shown how to obtain inductive circuit parameters by innovative measurement on an actual machine and how results from simulation compare to laboratory testing. The resulting “complete” model is more logical than conventionally used equivalent circuits and aid in understanding of the principles of DC machines.*

Key words: *DC machine, circuit model, inductance, SIMULINK.*

1. Introduction

The need for Engineers to understand the principles of electric machines is growing as electric machines pervade the modern world. The currently occurring metamorphosis of the automobile engine, a traditional symbol of Mechanical engineering, into an electric machine is just one striking example. For educational institutions in particular there is a corresponding need to thoroughly educate students with the relevant principles of electric machines, and this is typically done with the aid of suitable analysis, modelling and simulation tools, including the traditional approach of using simple equivalent circuits to aid in understanding and analysis of electric machine performance. While the traditional approach has merit in introducing the topic, it is unfortunately limited by the degree of correspondence to real machines. These simple equivalent circuits, as typically presented in textbooks, are the result of several decades of intuition by the pioneers of machine theory, and have embedded subtle simplifications. Consequently, the electric machine principles represented are limited by

the simplicity of these equivalent circuits and the lack of direct physical correspondence with typical machine structures.

Modern numerical techniques have the potential to enable much more realistic models to be developed, and finite-element modelling is the approach of choice for giving potentially excellent correspondence with experimental measurements. These models can include detail of physical construction and can be solved over time to accurately simulate dynamic effects such as those resulting from system inertia, changes in the supply and varying load conditions. While such numerical techniques can be used to good effect in advanced analysis, they are limited in intuitively exposing the relationship between elements of a machine structure and the corresponding measured electric characteristics.

Our approach to bridging the gap between overly simplistic equivalent circuits and “non-intuitive” numerical models is in hybrid models. We propose that these utilise more complete equivalent circuits that intuitively correspond to the physical machine and are solved numerically enabling temporal dynamic effects such as those due to commutation to be incorporated.

Our focus is primarily on DC machines of which we have had a particular interest. For example, we previously derived a DC motor equivalent circuit model that could include a short-circuit fault in an armature coil and be used in studies of condition monitoring of electric machines [1]. This model considered each physical electrical coil in the motor and associated current loops and comprised a series of resulting differential equations that were subsequently solved for the armature and field currents in the coils. This motor model improved on traditional equivalent circuits but had limitations. Interestingly, at the time, the computation of one

second of motor currents took one whole day of processing, due to both inefficient model implementation and the use of relatively slow PCs. Also, agreement between predicted and measured currents, both in waveform and amplitude, was rather poor, due to complexities of the machine, such as mutual inductance between coils that were not adequately modelled. It was apparent that it is very important to take adequate account of magnetic saturation and inductive coupling and also to correctly measure the inductances associated with the various current loops in the equivalent circuits.

Here, as an example of a hybrid approach of combining a realistic equivalent circuit and a numerical simulation solution, we describe the further development of this original model and its new implementation in SIMULINK (Mathworks, USA) for a particular example DC motor. We describe the experimental methods used for the measurement of coil inductance, the mathematical model, the SIMULINK implementation, and the comparison of modelled armature and field current waveforms with measured waveforms in the real machine.

2. Circuit model

The circuit model was based on a relatively complex set of equivalent circuits representing each temporal state of the machine. The approach taken was to implement equations for current loops corresponding to the physical coils in the machine. Model implementation therefore depended on machine configuration. The following model development is for a specific DC machine in our laboratory, a $\frac{1}{2}$ HP, 1440 rpm, 180 Volt DC motor manufactured by F.W. Davey & Co., Melbourne, Australia (the “Davey machine”). Its main features (Fig. 1) were a conventional armature that was lap wound with 48 coils in 16 slots (3 coils per slot), with connections from these coils to 48 segments on the commutator, and a separately excited 2-pole field winding. Each brush spanned about 30° and made contact with alternately 4 or 5 commutator segments as the armature rotated.

The armature winding was initially modelled as 48 coils [3]. However, inductive coupling between coils sharing a slot was measured as extremely close to unity, leading to numerical singularities during solution of the circuit equations. This problem was overcome in the modelling by combining each set of three coils in the same slot into one coil. The effective armature winding therefore consisted of 16 coils connected to 16 commutator segments, with each segment occupying 22.5° (ignoring insulation between segments). Measurements of coil inductance had of course to allow for this.

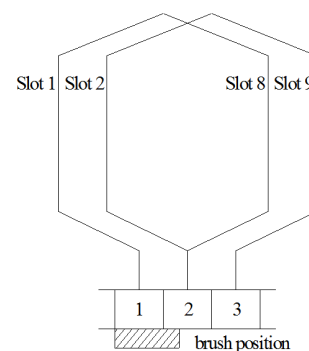


Fig. 1 Davey machine armature: as the coils move past the brush, one and then two coils are shorted by the brush.

3. Equivalent circuits seen during operation

There were 6 equivalent circuits for the armature (from 6 armature circuit loops) and 1 for the field.

Armature loop 1: Fig. 1 shows two coils connected to three segments and is drawn in a conventional “developed winding” style. The coil with sides in slots 1 and 8 was connected to segments 1 and 2 and was shorted by the brush in the position shown. When the armature had moved a few degrees to the left, the brush contacted segments 1, 2, and 3 and thus shorted two coils. After a few more degrees the brush contacted only segments 2 and 3 and thus shorted only one coil again. The model therefore switched between equivalent circuits, depending on whether a brush contacted two or three segments during commutation.

Armature loop 2: Fig. 2 has a different style, showing all the coils, and this helps to explain the 7-coil equivalent circuit of Fig. 3. Fig. 2 shows each

brush shorting out two coils. The segments have been omitted but the numbers 1 to 16 correspond to them.

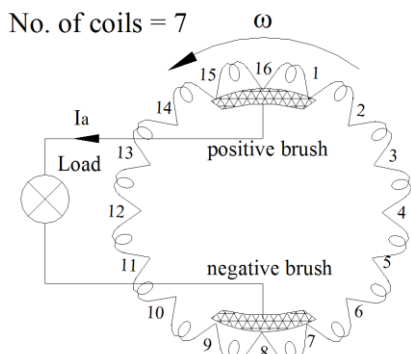


Fig. 2 Alternative way to show the armature coils and brushes for the 7-coil circuit

Armature loop 3: In Fig. 3, the loops containing currents i_1 and i_2 include the two sub-coils being commutated under the positive brush. Current i_1 is in the coil connected to segments 15 and 16, and i_2 is in the coil connected to segments 16 and 1. Loops containing currents i_3 and i_4 are for the negative brush. Currents i_5 and i_6 flow through coils L_{S1} and L_{S2} , which are each the series connection of six coils, connected between segments 15 and 9, and segments 1 and 7, respectively. The total armature current is $i_5 + i_6$. Current i_f is in the separately-excited field coil L_f . R_{p1} , R_{p2} and R_{p3} are positive brush resistances (see later), and R_L is the load resistance.

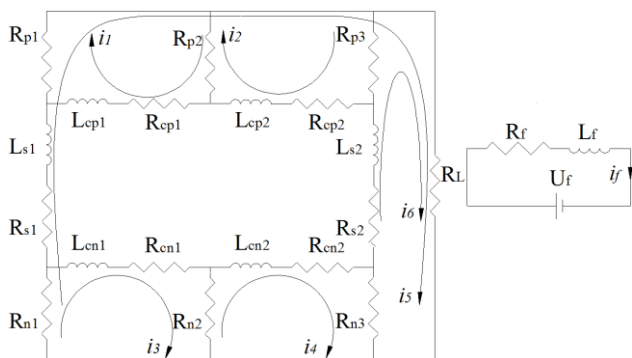


Fig. 3 The 7-coil equivalent circuit

Armature loop 4: In Fig. 4 each brush shorts out one coil and this corresponds to the 5-coil equivalent circuit of Fig. 5 which contains five current loops. Current i_1 flows in one coil connected to segments 16 and 1 that is shorted by the positive brush. Current i_2 is in the coil connected to segments 8 and 9 that is shorted by the negative brush. Currents i_3 and i_4 flow

through coils L_{S1} and L_{S2} , each of which contain 7 coils in series, connected between segments 16 and 9, and between 1 and 8, respectively.

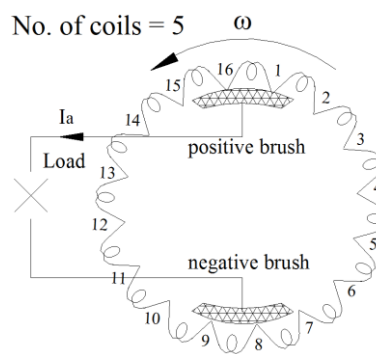


Fig. 4 Armature coils and brushes for the 5-coil equivalent circuit

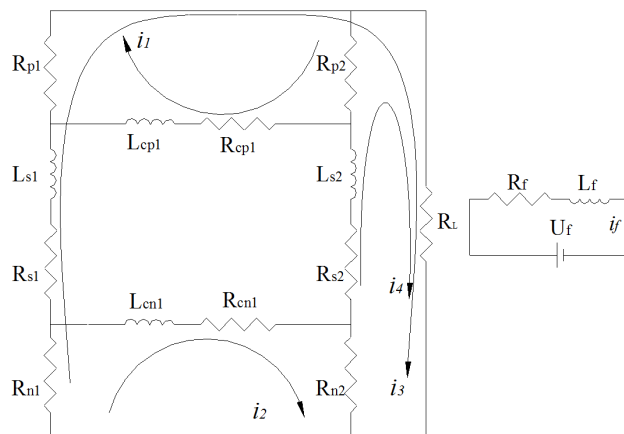


Fig. 5 The 5-coil equivalent circuit

Armature loop 5: Fig. 6 enables the duration, in degrees of rotation, of the 7-coil and the 5-coil circuits to be calculated, as follows. Fig. 6(a) shows each brush shorting one coil. (Assume that the *right* hand edge of each brush is opposite a very thin piece of insulation between commutator segments so that the brush does not contact the segment to the right of that edge). Fig. 6(c) shows the *left* hand edges of each brush now opposite the commutator insulation. The armature has rotated $(30 - 22.5) = 7.5$ degrees. Any rotation in between these corresponds to a 7-coil equivalent circuit, Fig. 6(b). It follows that the 5-coil circuit lasts for 15 degrees of rotation, and the 7-coil circuit for 7.5 degrees.

Field loop: The field loop did not vary over time and is shown in both Figs. 3 and 5.

Brush resistance: Fig. 6 also shows how we presume that the brush resistance alternates between two resistors in parallel for the 5-coil circuit and

three resistors in parallel for the 7-coil circuit. The value of every resistor varies continuously with armature position.

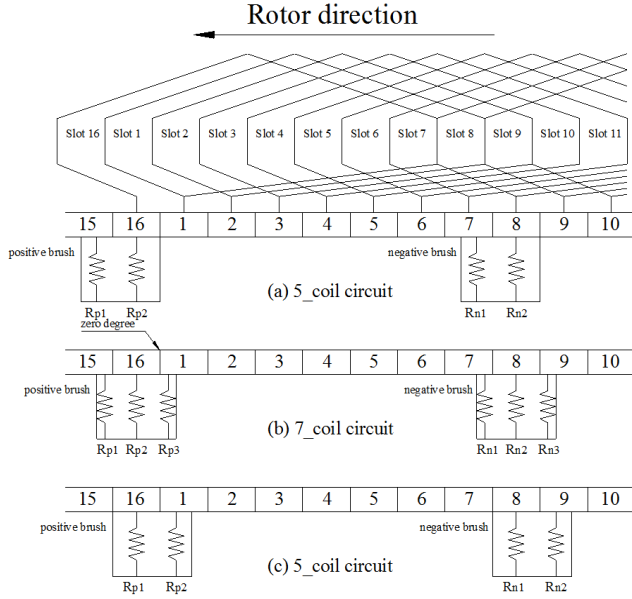


Fig 6. Diagram used in the calculation of the duration of the shorting out of (a) and (c) one coil, and (b) two coils

4. Loop voltage equations

Since we originally required current waveforms for condition monitoring purposes, and these would be near enough identical for a particular machine whether motoring or generating, we chose to model a generator rather than a motor because torque terms are not needed, and the speed can be set independently.

The voltage equations (1) can be written for the 7-coil equivalent circuit of Fig. 3, using the usual conventions. The 7 loop currents are the dependent variables i_1 to i_6 and i_f .

The symbols are defined as follows:

L_{CP1} and L_{CP2} are self inductances of the coils under the positive brush in loops 1 and 2.

L_{CN1} and L_{CN2} are self inductances of the coils under the negative brush in loops 3 and 4.

L_{S1} and L_{S2} are self inductances of the 6 non-commutated coils in series in loops 5 and 6.

L_f = Self inductance of the field circuit.

$M_{ij} = M_{ji}$ = Mutual inductance between the coils in loop i and loop j .

M_{if} = Mutual inductance between the coils in loop i and the field.

M_{66} = Mutual inductance between the parallel paths in loop 5 and loop 6.

ω_r = Machine rated speed.

R_{S1} and R_{S2} are the resistances of the 6 non-commutated coils in series.

R_{p1} , R_{p2} , R_{p3} , R_{n1} , R_{n2} and R_{n3} are the positive and negative brush resistances.

R_{Cp1} , R_{Cp2} , R_{Cn1} and R_{Cn2} are the coil resistances under the positive and negative brushes.

$$\begin{aligned}
\text{Loop 1: } 0 &= i_1 (R_{p1} + R_{p2} + R_{CP1}) + i_5 R_{p1} - i_2 R_{p2} + M_{12} \frac{di_2}{dt} - M_{13} \frac{di_3}{dt} - M_{14} \frac{di_4}{dt} - M_{1f} \frac{di_f}{dt} + L_{CP1} \frac{di_1}{dt} \\
\text{Loop 2: } 0 &= i_2 (R_{p2} + R_{p3} + R_{CP2}) - i_6 R_{p3} - i_1 R_{p2} + M_{21} \frac{di_1}{dt} - M_{23} \frac{di_3}{dt} - M_{24} \frac{di_4}{dt} - M_{2f} \frac{di_f}{dt} + L_{CP2} \frac{di_2}{dt} \\
\text{Loop 3: } 0 &= i_3 (R_{N1} + R_{N2} + R_{CN1}) + i_5 R_{N1} - i_4 R_{N2} - M_{31} \frac{di_1}{dt} - M_{32} \frac{di_2}{dt} + M_{34} \frac{di_4}{dt} + M_{3f} \frac{di_f}{dt} + L_{CN1} \frac{di_3}{dt} \\
\text{Loop 4: } 0 &= i_4 (R_{N2} + R_{N3} + R_{CN2}) - i_6 R_{N3} - i_3 R_{N2} - M_{41} \frac{di_1}{dt} - M_{42} \frac{di_2}{dt} + M_{43} \frac{di_3}{dt} + M_{4f} \frac{di_f}{dt} + L_{CN2} \frac{di_4}{dt} \\
\text{Loop 5: } 0 &= i_5 (R_{p1} + R_{N1} + R_{S1} + R_L) + i_1 R_{p1} + i_3 R_{N1} + i_6 R_L + M_{66} \frac{di_6}{dt} + k \cdot i_f \omega_r + L_{S1} \frac{di_5}{dt} \\
\text{Loop 6: } 0 &= i_6 (R_{p3} + R_{N3} + R_{S2} + R_L) + i_2 R_{p3} - i_4 R_{N3} + i_5 R_L + M_{66} \frac{di_5}{dt} + k \cdot i_f \omega_r + L_{S2} \frac{di_6}{dt} \\
\text{Field Loop: } U_f &= i_f R_f + M_{1f} \frac{di_1}{dt} + M_{2f} \frac{di_2}{dt} - M_{3f} \frac{di_3}{dt} - M_{4f} \frac{di_4}{dt} + L_f \frac{di_f}{dt}
\end{aligned} \tag{1}$$

Since each loop contains only one coil there is only one self-inductance term in each equation. However the mutual inductances, and in particular their signs, need close attention.

Fig. 7 shows the field coils on the horizontal or field axis. The armature sub-coils are drawn such that the direction of the coil axis is the same as the direction of MMF due to current in that coil. The corresponding flux direction is not the same because of the shape of the magnetic field structure. However, the commutator action makes it possible to assign clear directions to the flux produced by relevant groups of armature coils, as follows. Coils connected to segments 15-16 and 16-1 are under the positive brush. Current in them produces flux in the field axis. Ditto for the coils 7-8 and 8-9 shorted by the negative brush. The remaining coils are in two groups between segments 1 to 7 and 9 to 15. Currents in them produce resultant flux in the vertical direction, or armature axis.

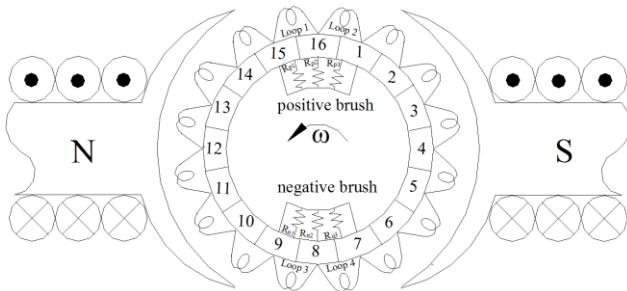


Fig. 7 Armature and field coils in the correct MMF directions relative to each other

In Fig. 3, loops 1, 2, 3 and 4 have mutual inductance with each other, as denoted by M_{12} , M_{13} , M_{14} , M_{23} ... to M_{43} . They also have mutual inductance of M_{1f} , M_{2f} , etc, with the field. There is no flux linkage between loops (1 and 3) and loops (5 and 6), so their mutual inductances are all zero.

The two groups of six non-commutated armature coils have mutual inductance with each other, denoted as M_{66} in both loops 5 and 6. They have zero mutual inductance with the field coils.

The signs of the mutual inductances of the coils undergoing commutation can be determined with the help of Fig. 8 which is a modification of the 7-coil circuit. These coils have been drawn encircling a fictitious steel bar so that the directions of the flux

that their currents produce are more obvious than in Fig. 3 (the load resistor R_L and the field loop are not included). The mutual inductances with a minus sign in the loop equations are those between (loops 1 and 2) with (loops 3 and 4), and (loops 1 and 2) with the field loop. In the field circuit, the minus signs of the mutual inductances are only associated with loops 3 and 4. The remainder of other mutual inductances have a plus sign.

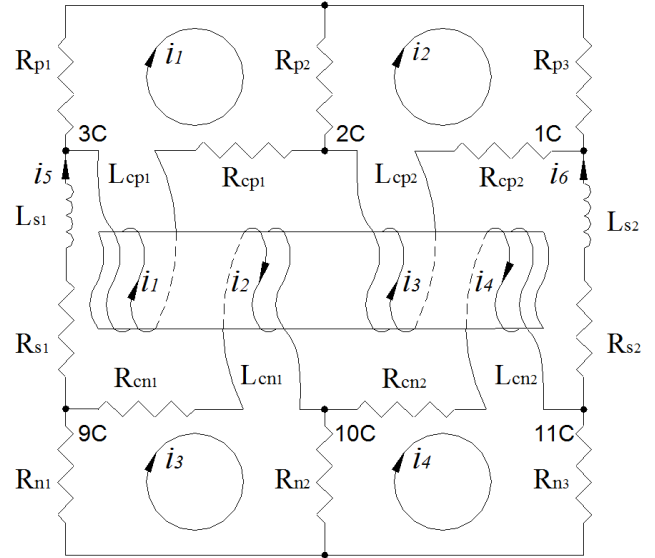


Fig. 8 MMF directions for the calculations of mutual inductances of the 7-coil equivalent circuit

The equations for loops 5 and 6 both contain the term $k i_f \omega_r$, which is recognizable as the open-circuit armature voltage. It is a generator voltage, produced by the motion of coils L_{s1} and L_{s2} at right angles to the constant field flux. By contrast, all the $L di/dt$ and $M di/dt$ terms are transformer voltages produced by time-varying flux.

Similar sets of equations exist for the 5-coil circuit but have not been included in order to save space.

5. Measurement of inductances

Inductances needed to be measured under magnetic flux conditions equivalent to those in the motor under normal operation. This required a constant (rated) current of 0.2A in the field coils, and rated armature current.

The usual method of measuring inductance is to use an alternating supply (often 1000Hz) to the

inductance, measure the current and voltage, and calculate the impedance to obtain both real and imaginary parts. A typical laboratory impedance meter does this. However, this AC method would give inaccurate results on the Davey machine even using 50Hz instead of 1000Hz because the closed field circuit would reduce the inductive part of the impedance being measured by an unknown amount. Our measurement of inductance was therefore based on the method of Jones [4] which effectively measures a DC inductance.

The circuits in Figs 9 (a) and (b) measure self inductance and mutual inductance, respectively. The bridge is first balanced so that $V = 0$. The supply is then removed by opening the switch. The measured self-inductance in Fig. 9 (a) is obtained from

$$L_1 = \frac{1 + R_1 / R_2}{i_1} \int_0^{\infty} V dt$$

and mutual inductance in Fig. 9 (b) from

$$M = \frac{1 + R_1 / R_2}{i_1} \int_0^{\infty} V_2 dt .$$

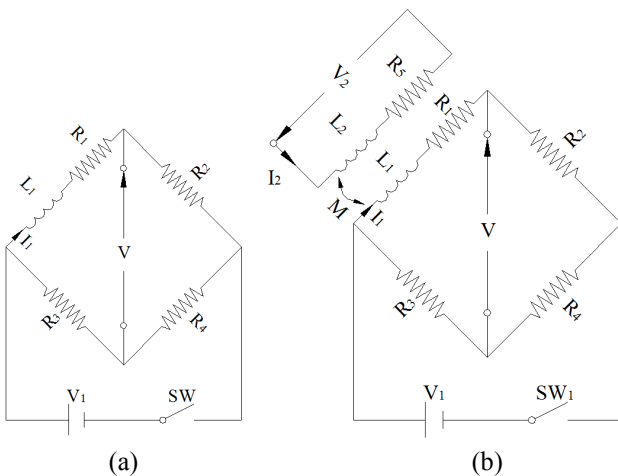


Fig. 9 Circuits for the measurement of (a) self and (b) mutual inductance

These equations are derived in appendix A, which also shows that any other inductively coupled circuits have no effect on the calculation of inductance. In fact, a dramatic demonstration of this method is to measure the inductance at the primary terminals of a transformer with a short-circuited secondary. The open circuit (or magnetizing) inductance is measured. An AC method would give the short-circuit inductance which is typically one thousand times less.

To prepare the motor for such measurements, the brushes were removed and extra connections made to every third one of the 48 commutator segments, ie to 16 segments.

The self-inductance of the six non-commutated sub-coils in series for the 7-coil circuit (ie, L_{s1} and L_{s2} in Fig. 3) were measured using the connection to the inductance bridge shown in Fig. 10. The series connected coils between segments 1-7 and 9-15 each had a 1A current flowing through them from the supply V_1 , and the inductance bridge measured the self-inductance of the two sets of six sub-coils in parallel. (We preferred in this way to maintain the symmetry of the flux pattern rather than measure the inductance of one set of six sub-coils). There was of course mutual inductance between the two sets of coils, but since the two sets occupied the same slots this mutual would be almost the same as the self inductance. The self inductance calculated from the integrated voltage was divided by 2 to give the value for one set of coils (after also allowing for the doubling effect of the reversal of current during the measurement). As mentioned previously, the field circuit carried 0.2A.

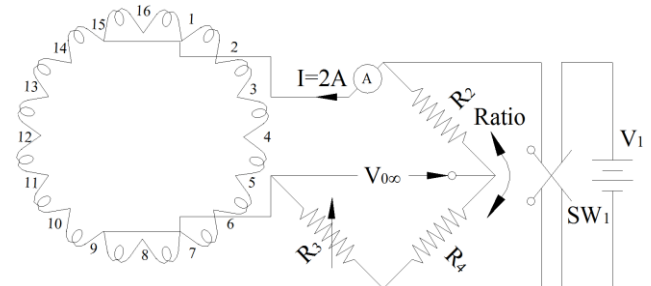


Fig. 10 The connections for measurement of the self inductance of series-connected armature coils L_{s1} and L_{s2} in the 7-coil equivalent circuit

Preliminary tests showed (a) that the measured self-inductance of the complete armature was more or less independent of the armature current for values between 1A and 3A, and (b) that about 5A of armature current produced the same flux as 0.2A in the field coils. Rated load current was 3.2A, so we used a total current of 2A for all inductance measurements, ie. 1A in each of the two coils in parallel.

The circuit in Fig. 11 is for measuring the mutual inductance M_{12} between the two coils under the

positive brush.

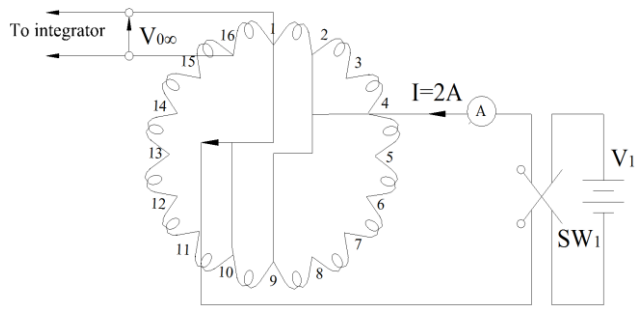


Fig. 11 The connections for the measurement of the mutual inductance between two armature coils for the 7-coil equivalent circuit

A somewhat special case was measurement of the self-inductance of the field coils. The current in this is not exactly constant but has a small ripple at the commutator frequency – a result of the mutual inductance between the field winding and the armature coils, and the switching action of the commutator. Measurement of the field current showed typically a peak to peak ripple of about 5%. We needed an incremental self-inductance to relate to this ripple. Thus the field self-inductance should not be measured by integration of the bridge voltage during the reversal of the 0.2A field current, but by integrating the bridge voltage whilst the field current was reduced from 0.2A to 0.19A.

Although this section is all about inductances, the coil resistances deserve a mention.

Armature coil resistances were of the order of one or two ohms, and were measured with a digital microhm-meter. Due to the expected small effect of the resistances on the current waveforms, precise values were not necessary, and temperature correction was not made.

6. Resistances

Measurement of brush resistance was not attempted. Instead, a brush resistance model with a 1.0 V drop across each brush was assumed, which meant that the resistance of a portion of the brush was inversely proportional to the area of the brush in contact with a particular segment of the commutator. Hence, the conductance of the whole brush was obtained from $G_W = (\text{rated current})/(\text{total voltage drop on the brush}) = 3.2\text{A}/1\text{V} = 3.2$ Siemen. For example, for the 7-coil circuit, the brush

conductances for the three resistors shown “inside” the positive brush in Fig. 6b were calculated as follows:

$$G_1 = \frac{d_1}{W} G_W, \quad G_2 = \frac{d_2}{W} G_W, \quad G_3 = \frac{d_3}{W} G_W,$$

where d_x ($x = 1, 2, \text{ or } 3$) is the contact length between segment x and the portion of the brush in degrees, W is the brush width (30°), and $G_W = 3.2$ Siemen. Consequently, brush resistances R_{pi} and R_{ni} varied continuously with rotor position.

7. Numerical Solution

The complete model [2] of the Davey machine was implemented in SIMULINK. Simulation of the performance of the machine was done by solving the model sequentially with a time step of $116 \mu\text{s}$ (equivalent to a 1° rotor rotation at 1440 r/min), an initial armature current of zero, and an initial field current of 0.2 A. Solution of the model was done using SIMULINK’s ODE4 solver. Simulations were run until the machine achieved steady state.

Time domain management and data flow during the simulation of the healthy machine may be summarized as follows. The starting position was arbitrarily taken to be during the 7 coil equivalent circuit. Commutation resulted in alternate switching between the 7 and 5 coil circuits. Because of the inductances in each loop, currents were modeled as continuous just before and after switching, ie. the final values of currents in circuit 7 became the initial values of currents in circuit 5, and vice versa. A complication was that there were two more currents loops in the 7-coil circuit, and we had to assume that these two currents became zero as the 7-coil circuit switched to the 5-coil circuit.

A technical consideration of SIMULINK required that the 7-coil and 5-coil equivalent circuits be re-written to locate the self-inductance of each loop on the right side of the individual loop equations. The reason for this was to be able to configure the SIMULINK model as shown in Fig. 12, with the output of the sum block being $L(di/dt)$. This then allowed the addition of a time delay (equivalent to a 1 degree rotation of the machine) and integrator to the feedback signal to get the loop current i .

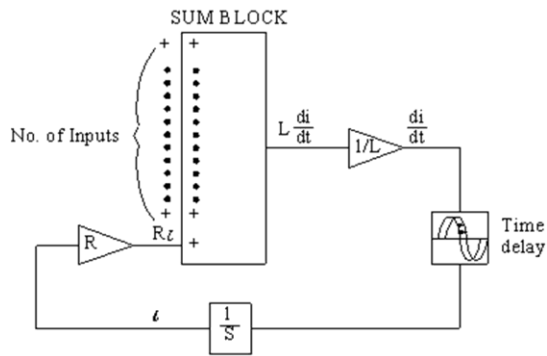


Fig. 12 SIMULINK sum block used in the solution of the voltage equations

8. Simulation results

The simulation could be computed in real-time and produced results useful for illustrating the electric machine principles. Fig. 13 shows predicted waveforms of (a) armature current I_a and (b) field current I_f with the zero of the y-axis suppressed in order to show the ripples clearly. The frequency of the ripple is about 380 Hz, which relates closely to the theoretical commutator frequency of $16 \times 24 \text{ rev/sec} = 384 \text{ Hz}$. The peak to peak ripple is about 0.14A for the armature and about 3mA for the field current.

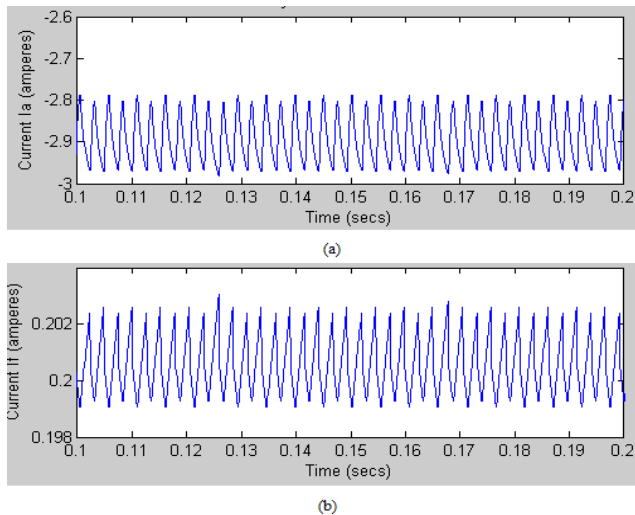


Fig.13 Predicted steady state (a) armature and (b) field currents for the Davey machine

Fig. 14a shows the measured waveform of the armature current. Ripple frequency is about 365Hz, which is rather less than the expected 384 Hz. In retrospect, we realize that the Davey machine was driven by an induction motor from a variable frequency supply set at 48 Hz (4 pole induction

motor) and of course the motor's rotor would be a bit slower than 24 rev/sec. The peak to peak ripple is about 0.26A. Note that the ripple is not at $48 \times 24 = 1152 \text{ Hz}$ which would be expected for a 48 segment commutator, and thus in this respect it justifies our model with 16 segments.

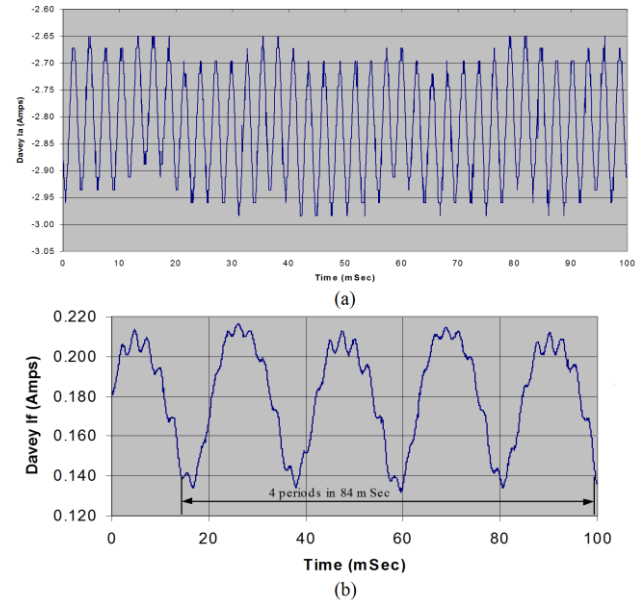


Fig.14 Measured steady state (a) armature and (b) field currents for the Davey machine

Fig. 14b shows the measured waveform of the field current, which was somewhat of a surprise. The large-amplitude ripple is about 48 Hz which is twice the speed of the generator. This may be due to a slightly oval armature – an imperfection of the real world!

Superimposed on this is a much smaller ripple which is at the commutator frequency. It is difficult to judge its amplitude with any accuracy but it is about 0.01A peak to peak.

The fact that the predicted ripples were about half the measured ripples suggested errors in measured inductances and/or resistances. We ran the simulation with all inductances firstly doubled and then halved. The former gave roughly half the ripple and the latter roughly double the ripple, so it looked as if the measured inductances were too high. Since the ripple results from the switching between one and two shorted coils, an error in the self and mutual inductances of these coils would be the likely cause, and unfortunately the error was of the order of tens of percent for these relatively low inductances.

9. Conclusions

The more realistic modelling approach presented here compliments traditional equivalent circuits of DC machines and provides an illuminating insight into the "real" operation that is the basis of operation of all modern electric machines.

This circuit model is more intuitive than the conventional equivalent circuit; it does not lump all the armature coils into just one coil, and can naturally demonstrate the switching action of commutation. In fact, we have repeatedly found these features to be valuable instructional aspects for developing an understanding of DC motors and also electric machines in general.

The circuit model finds particular application in teaching that aims to give students a thorough understanding of the principles of DC machines, particularly the temporal current distributions in the armature coils and the effects of commutation, and complements the use of conventional equivalent circuits. In particular,

- all the visible coils are in the circuit model rather than the less easily justifiable single armature coil of the conventional equivalent circuit
- the measurement of coil inductance, both self and mutual, is in such a way as to take account of magnetic saturation
- the conventional equations of loop analysis of circuits are in the time domain.
- the solution of the differential equations is in SIMULINK
- there are both transformer and generator voltages in the loop equations
- there is a clear demonstration of commutation
- testing of the machine is done under rated operating conditions in order to record representative armature and field current waveforms.

References

- [1] S.Y.S. Ho and R.A. Langman, 'The mathematical model of a DC motor', *Journal of Electrical and Electronic Engineering, Australia*, 22(2) (2003), 93-107.
- [2] N. Chuang, 'A mathematical model of a DC machine',

MEngSc thesis, University of Tasmania (2004).

- [3] S.Y.S. Ho, 'Condition monitoring of Electrical machines', PhD thesis, University of Tasmania (1998).

- [4] C.V. Jones, *The Unified Theory of Electrical Machines* (Butterworths, London, 1967).